ARTICLE

New heterometallic Co/Zn, Ag/Co, and Ag/Zn imidazolates: structural characterization and catalytic activity in the oxidation of organic compounds

Received 00th January 20xx,
Accepted 00th January 20xx

DOI: 10.1039/x0xx00000x

Mattia Lopresti[a], Łukasz Kurowski[b], Luca Palin[a], Marco Milanesio[a*], Magdalena Siedzielnik[b], Karolina Gutmańska[b], Adriana Dobrenko[b], Tomasz Klimczuk[c], Ewelina Pawelczyk[b,d], Anna Dołęga[b$]

a. aDipartimento di Scienze e Innovazione Tecnologica and CrisDi Interdepartmental Center for Crystallography, Università del Piemonte Orientale Viale T. Michel 11, 15121 Alessandria, Italy.
b. Department of Inorganic Chemistry, Chemical Faculty, Gdansk University of Technology, Narutowicza St. 11/12, 80-233, Gdańsk, Poland
c. Faculty of Applied Physics and Mathematics and Advanced Materials Centre, Gdansk University of Technology, Narutowicza St. 11/12, 80-233, Gdańsk, Poland.
d. d. Department of Process Engineering and Chemical Technology, Chemical Faculty, Gdansk University of Technology, Narutowicza St. 11/12, 80-233, Gdańsk, Poland
* E-mail: marco.milanesio@uniupo.it
$ E-mail: anna.dolega@pg.edu.pl

XRPD, SEM, EDX data, crystal structures

Table S1 Comparison of the bong lengths in **4c** and isomorphous zinc and cobalt imidazolates [Å].[25,64]

	4c M=Zn/Co	$ZnIm_2$ M=Zn	$CoIm_2$ M=Co
Ref.	This work	[64]	[25]
M-N	1.98172	1.79	1.938-
	1.98196	1.82	1.960
	1.98413	1.84	1.979
	1.98589	1.88	1.982
	1.99180	1.90	1.983
	1.99481	1.92	1.993
	2.00173	1.96	2.026
	2.00700	1.99	2.054
M···M*	5.924	-	5.905
	6.014	-	5.914
	6.021	-	6.003
	7.751	-	7.114

*Several shortest contacts between the atoms of metals in the crystal structure.

Table S2 Comparison of the bong lengths in **5**, **6** and their copper analogs [Å].[18,53]

	5	**6**	Cu_2ZnIm_4	Cu_2CoIm_4
Ref.	This work	This work	[18]	[53]
Zn-N	2.04936	-	1.990	-
Co-N	-	2.03843	-	1.991
Ag-N	2.05110	2.04446	-	-
Cu-N	-	-	1.886	1.869
Ag···Ag*	3.13619	3.10427	-	-
Cu···Cu*	-	-	3.109	3.153

*The shortest contacts between the atoms of metals in the crystal structure.

While substituted imidazoles (mostly methylimidazole) form ZiF-8 porous structure, metal-imidazole structures show dense forms based on a square-like arrangement of the metals in the asymmetric unit.[1,28,29,67] The replication of this square motif formed by imidazole-bonded metals, produces the skeleton of the crystal packing. This pattern can be recognized and characterized by the five metal-metal distances highlighted in the Figure S1 and reported in Table S3, where the three new structures **4c**, **5** and **6** are compared to some relevant monometallic compounds from the literature. This "square-like" motif grows into different patterns such as 2D layers in Ni-imidazolate or 3D-networks (compound **5**, **6** as well as cobalt[1] and nickel[28] imidazolates). Ag-imidazole (CCDC-603478[67]), interestingly, shows Ag dimers with a much shorter Ag-Ag contact, but then the square pattern can still be recognized, with similar distances to **5** and **6**, despite the different packing. Both **5** and **6**, show similar short Ag-Ag contacts but, instead of dimers, 1D rods of Ag are observed. As expected, in compound **6**, the metal-metal contact along the rod is shorter due to Co presence (Table S2). The arrangement of ZIF-62 (CCDC-

671070[29]) shows the two similar edges and a diagonal of about 8.8 Å, and 2-square edges with the diagonals of about 11 and 13 Å respectively. Compound **4c** adopts a similar arrangement but with deformations due to Co insertion. Pure Co imidazolate (CCDC 168799[1]) features much shorter distances. Newly reported compounds **5** and **6** show the edge distances in the basic square similar to that of pure Co but the edges of double square resemble the pure Ni compound (CCDC 211709[28]). Compound **6** features a shortest square diagonal, in agreement with the shorter atomic radius of Co with respect to Ag.

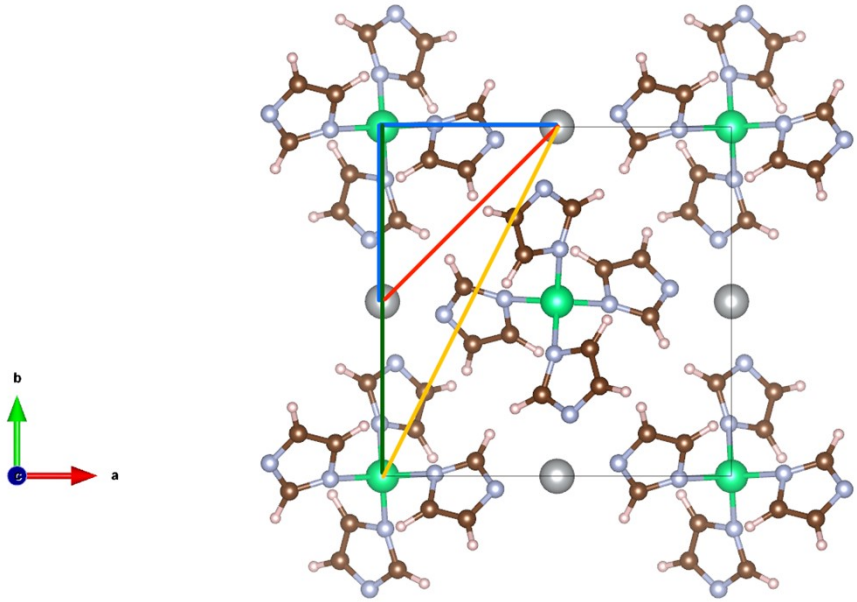

Figure S1 The crystal packing of **5** (green – Co, Grey – Ag). The structure is seen along *c* axis. Geometric parameters of crystal packing of the metal imidazolates analysed in the Table S3.

Table S3. Relevant geometric parameters (as defined in Figure S1) of **4c**, **5** and **6**, in comparison with literature data for the homometallic transition metal imidazolates.

Compd. M ratio and CCDC no.,[Ref.]. Geom. parameter	**4c*** **Co0.13Zn1.87** This work	**5** **Ag2Zn** This work	**6** **Ag2Co** This work	**Ag** 603478[67]	**Co** 168799[1]	**Zn*** (Zif-62) 671070[29]	**Ni** 211709[28]
Ag···Ag	----	3.136	3.104	3.139	---	---	----
Square edge 1 (Blue)	5.924, 6.014	6.051	6.027	6.208	5.989	5.968, 5.990	5.728
Square edge 2 (Blue)	6.021, 7.571	6.051	6.027	6.235	5.992	6.103, 7.729	5.728
Square diagonal (Red)	8.886, 8.888	9.048	8.004	7.425	7.964	8.531, 9.939	7.388
Two-square edges (green)	11.104	11.367	11.330	11.971	9.936	10.705	11.458
Two-squares diagonal (yellow)	13.315	12.877	12.833	12.035	10.110	13.703	11.915

* because of lower symmetry and thus larger asymmetric unit, all the four edges and two diagonals are reported

Refs.:
CCDC-603478: X.-C. Huang, J.-P. Zhang, X.-M. Chen CCDC 603478: Experimental Crystal Structure Determination, 2006, DOI: 10.5517/ccn7z1w
CCDC-168799: Y.-Q. Tian, C.-X. Cai, Y. Ji, X.-Z. You, S.-M. Peng, G.-H. Lee CCDC 168799: Experimental Crystal Structure Determination, 2002, DOI: 10.5517/cc5nn4l
CCDC-671070: R. Banerjee, A. Phan, B. Wang, C. Knobler, H. Furukawa, M. O'Keeffe, O. M. Yaghi, Science, 2008, **319**, 939, DOI: 10.1126/science.1152516
CCDC-211709: N. Masciocchi, F. Castelli, P. M. Forster, M. M. Tafoya, A. K. Cheetham, Inorg. Chem., 2003, **42**, 6147, DOI: 10.1021/ic034619o

FTIR spectroscopy

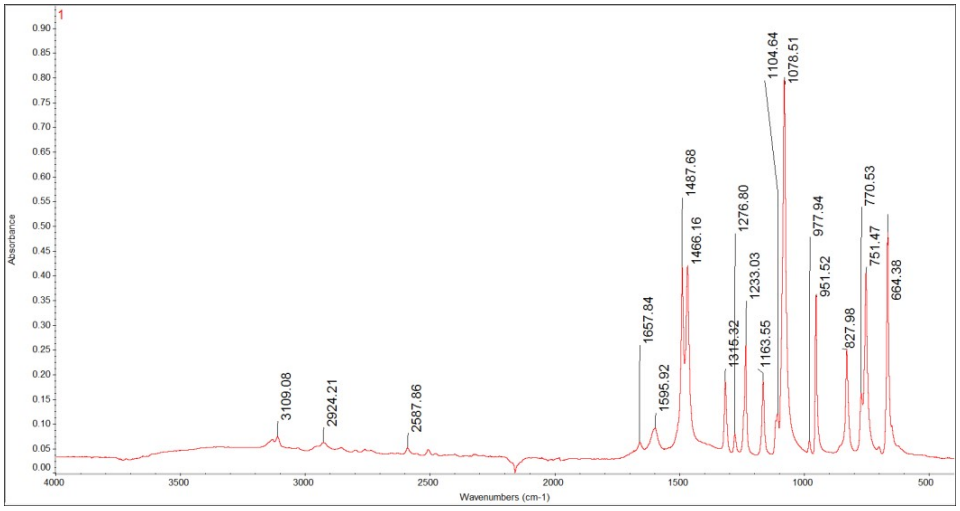

Fig. S2 The FT-IR ATR spectrum of **1**.

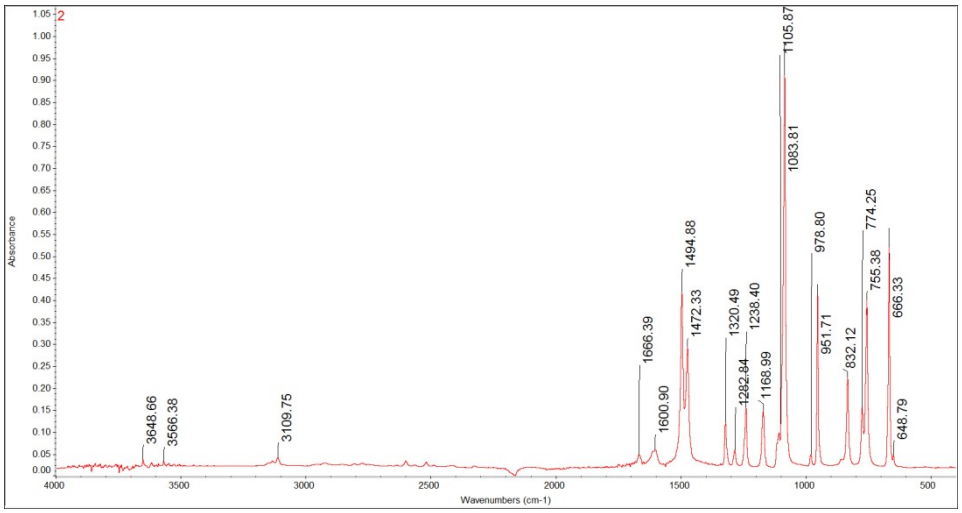

Fig. S3 The FT-IR ATR spectrum of **2**.

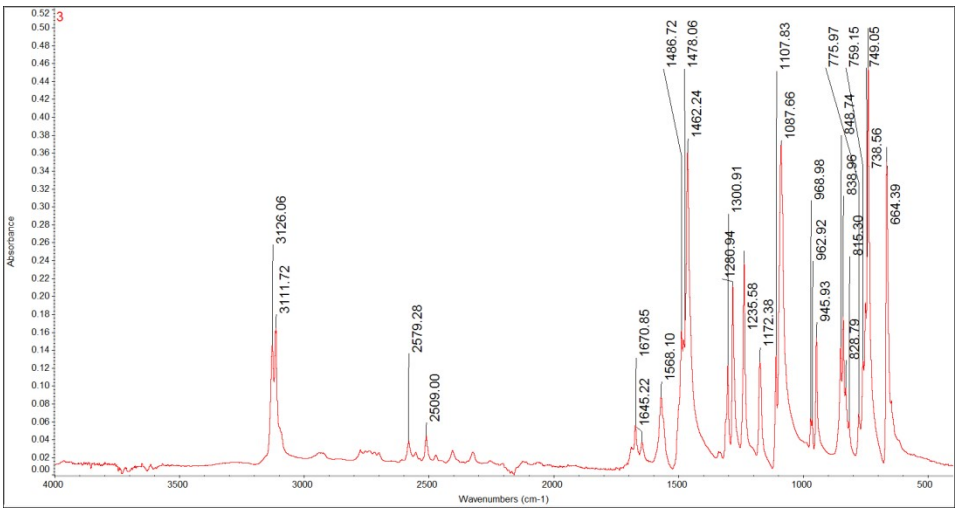

Fig. S4 The FT-IR ATR spectrum of **3**.

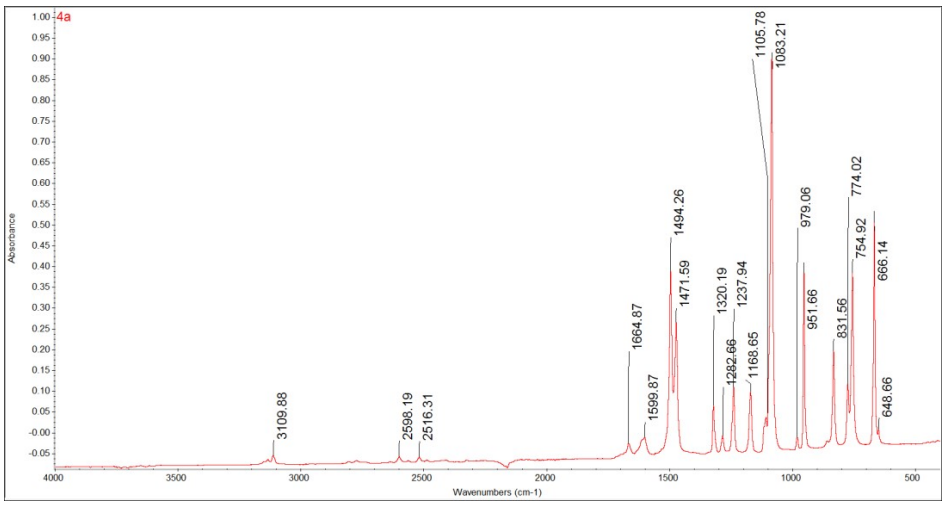

Fig. S5 The FT-IR ATR spectrum of **4a**.

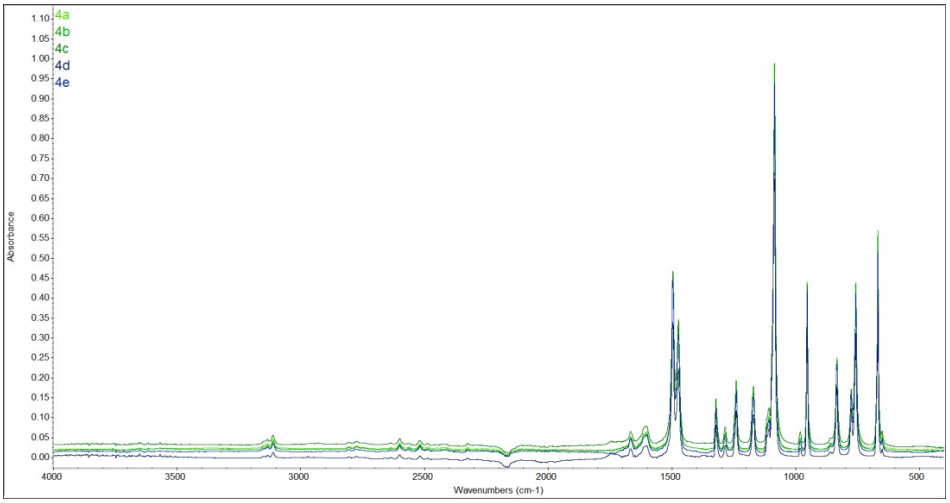

Fig. S6 The comparison of the FT-IR ATR spectra of **4a**-**4e** - full range.

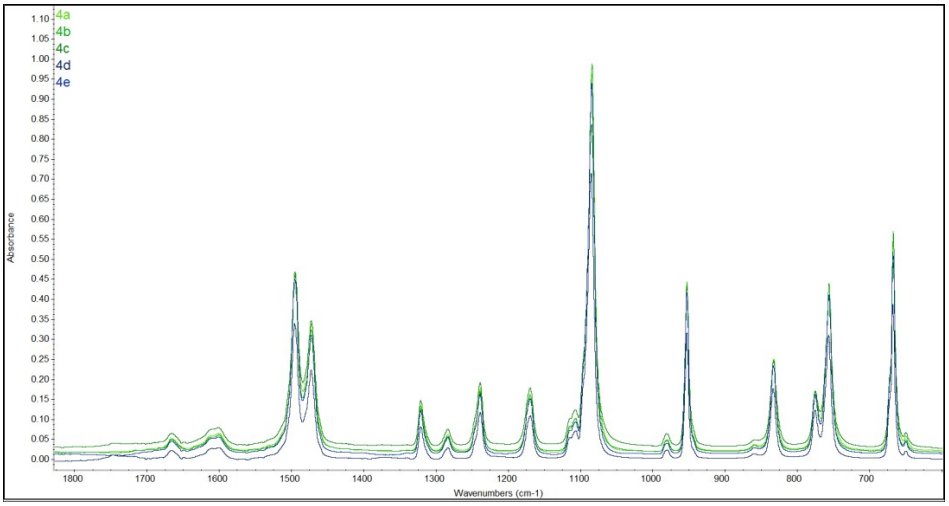

Fig. S7 The comparison of the FT-IR ATR spectra of **4a**-**4e** – finger-print range.

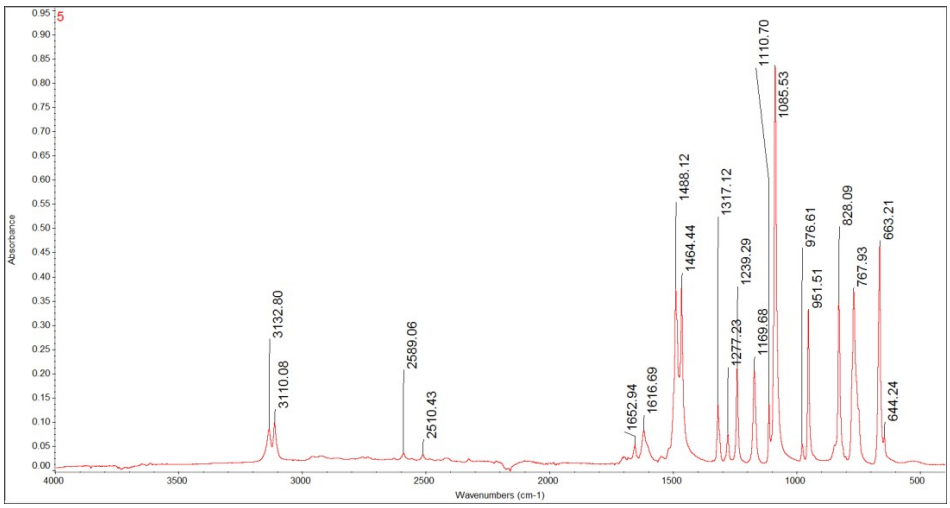

Fig. S8 The FT-IR spectrum of **5**.

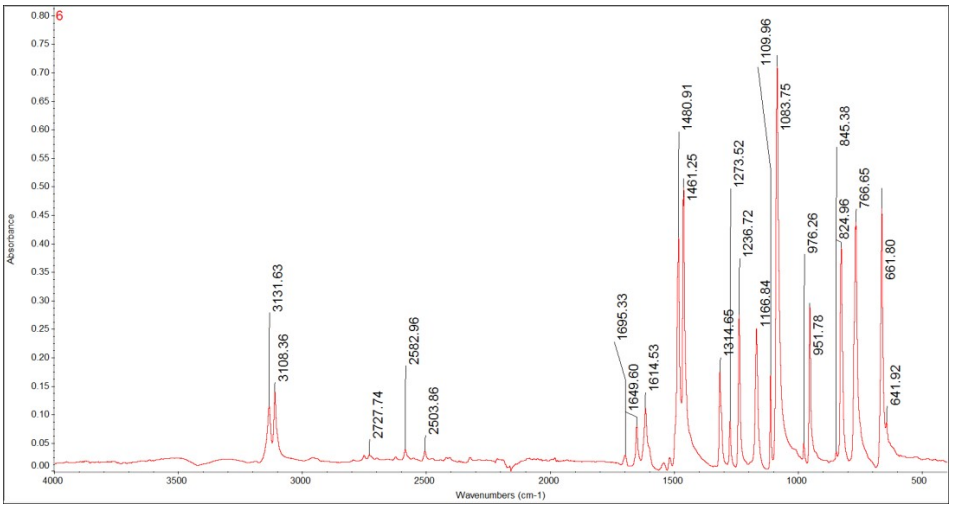

Fig. S9 The FT-IR spectrum of **6**.

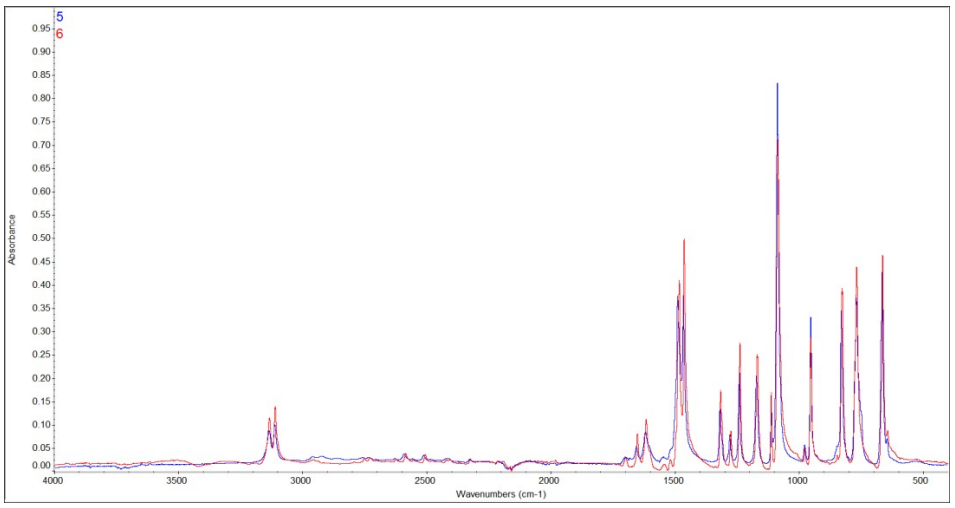

Fig. S10 The comparison of the FT-IR ATR spectra of **5** and **6** – full range.

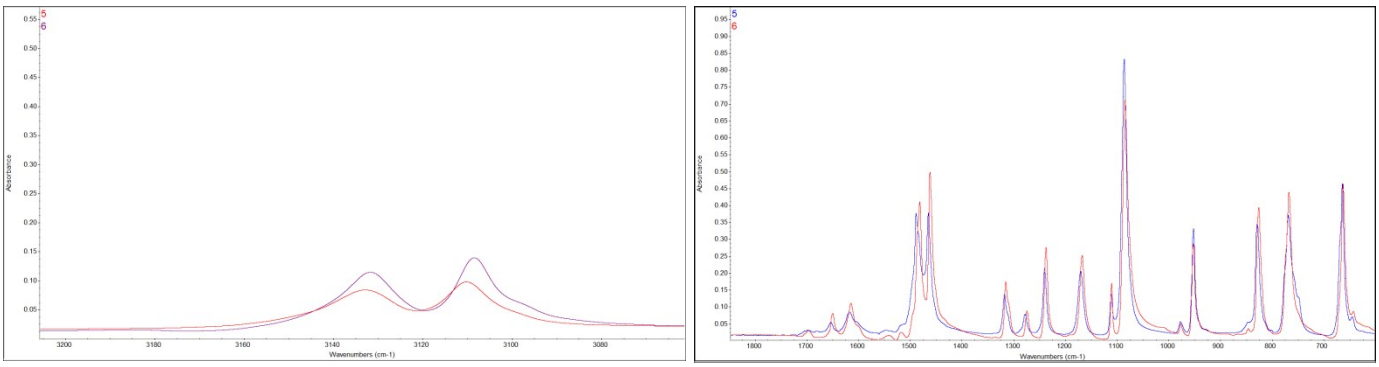

Fig. S11 The comparison of the FT-IR ATR spectra of **5** and **6** – CH stretching range (left side) and fingerprint range (right side).

UV-Vis – optical absorption properties

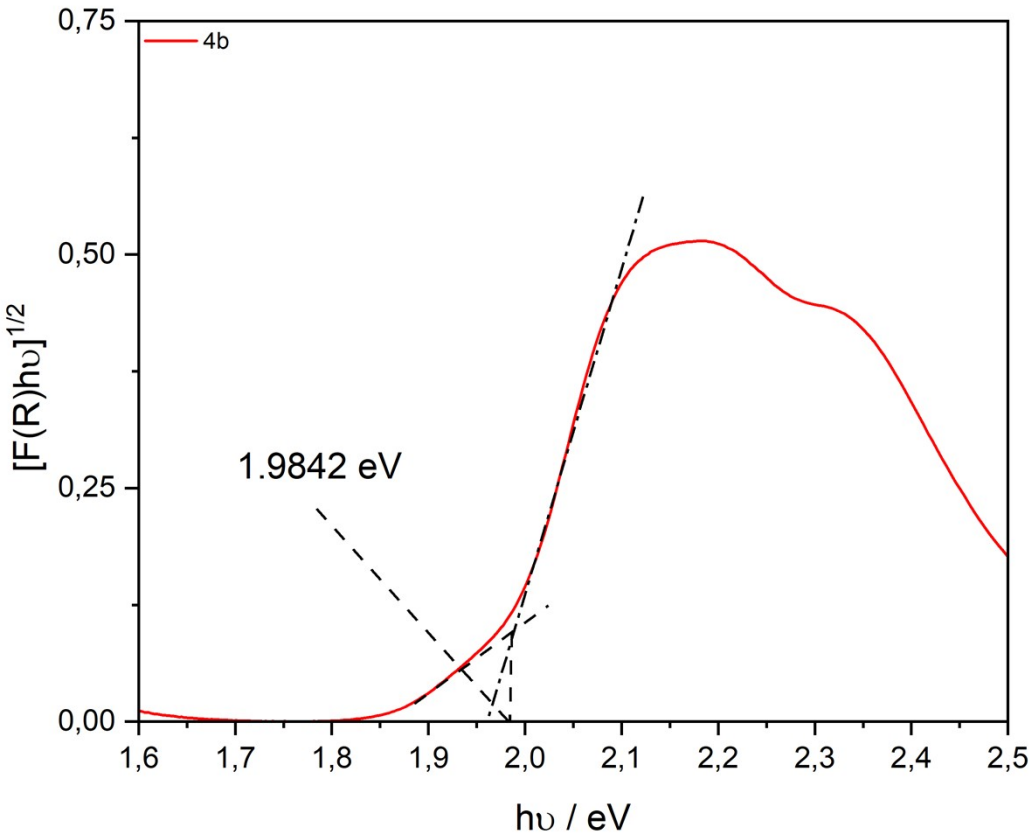

Figure S12. The Tauc plot of the **4b** sample. The first (recommended) method of determination of E_g is shown.

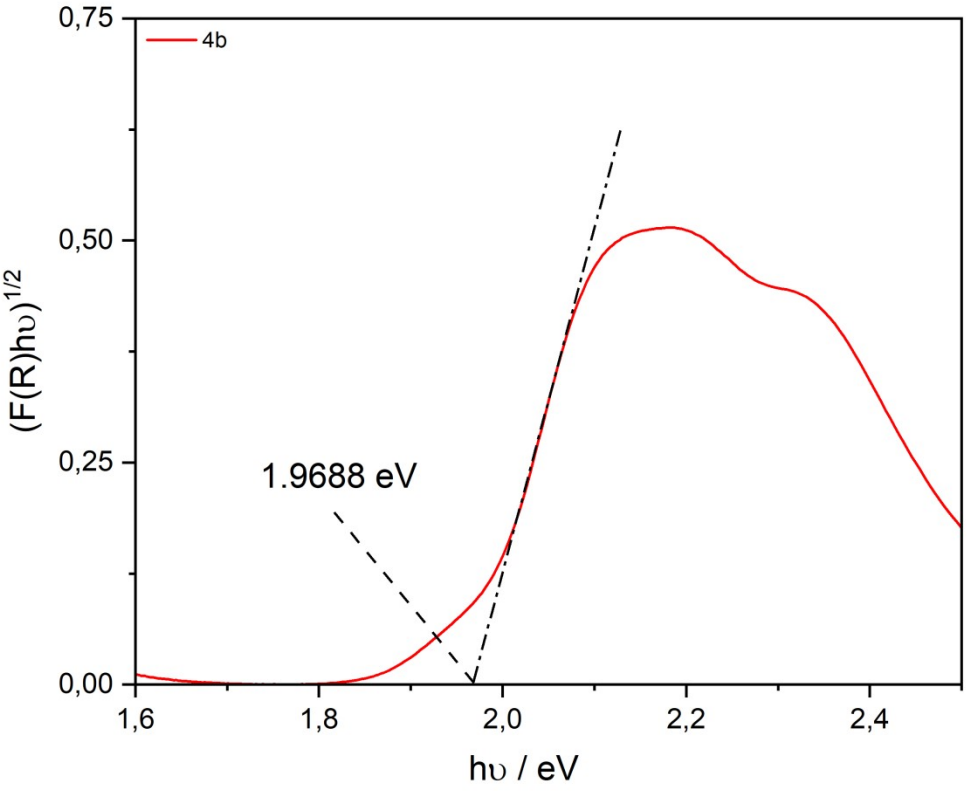

Figure S13. The Tauc plot of the **4b** sample. The second method of determination of E_g is shown.

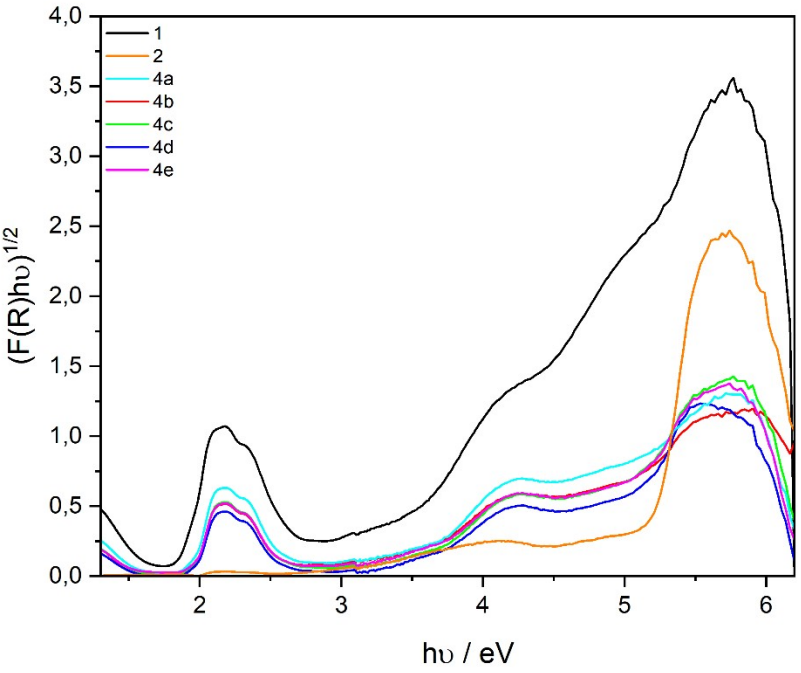

Figure S14. The Tauc plots of the samples **1**, **2**, **4a**-**4e** (full range).

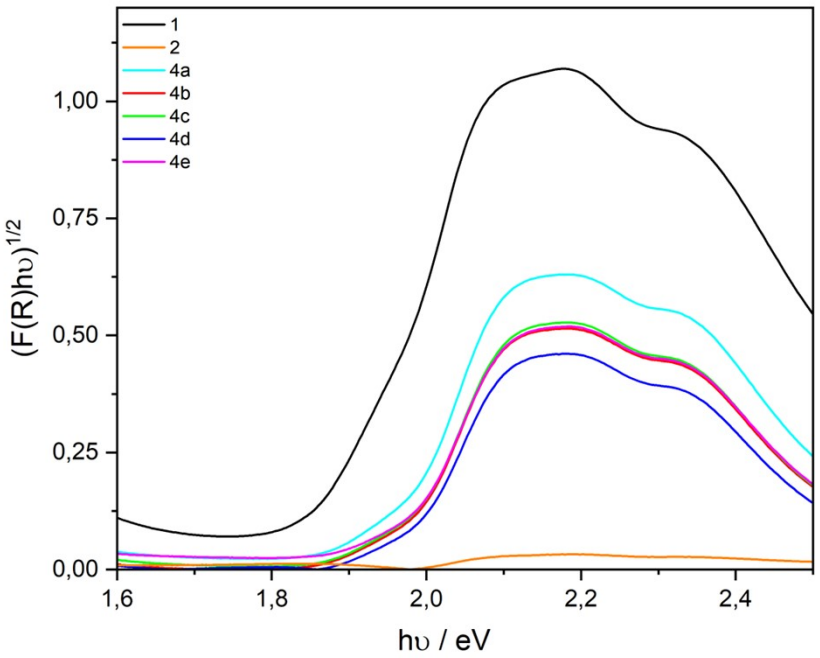

Figure S15. The Tauc plots of the **1**, **2**, **4a**-**4e** samples (Vis range).

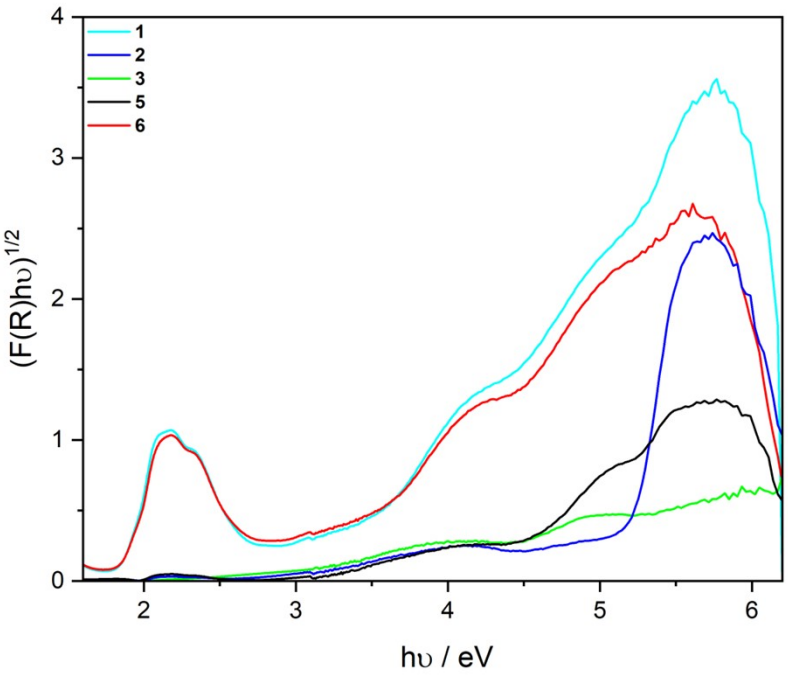

Figure S16. The Tauc plots of the samples: **1**-**3**, **5**, **6** (full range).

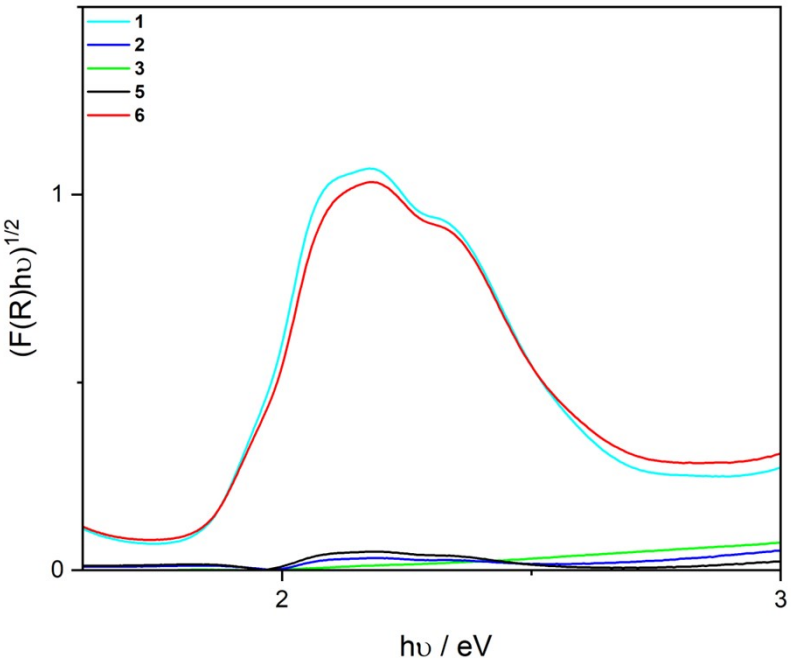

Figure S17. The Tauc plots of the samples: **1**-**3**, **5**, **6** (Vis range).

Table S4. Experimental E_g values obtained with different methods for $(F(R)hv)^{1/2}$.

Compound	Energy band gap [eV]	
	Tauc plot	Baseline approach
1	1.8659	1.9301
2	-	-
3	-	-
4a	1.9927	2.0237
4b	1.9688	1.9842
4c	1.9679	2.0000
4d	1.9694	1.9977
4e	1.9978	2.0260
5	-	-
6	1.8673	1.9479

Thermogravimetry of bimetallic imidazolates 4, 5, 6

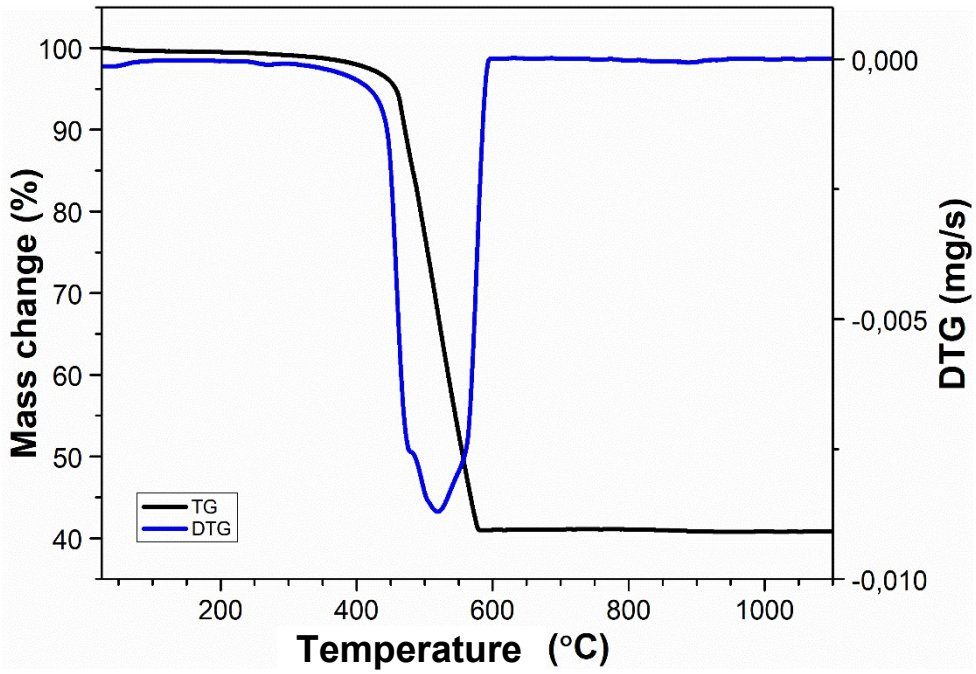

Figure S18. TG/DTG plot for **4a**.

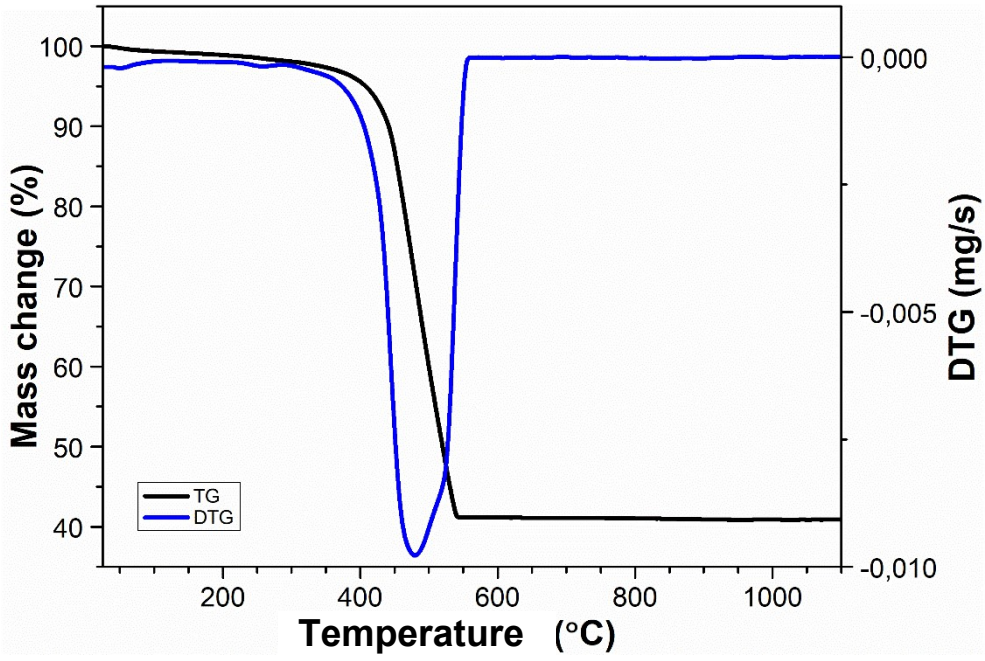

Figure S19. TG/DTG plot for **4c**.

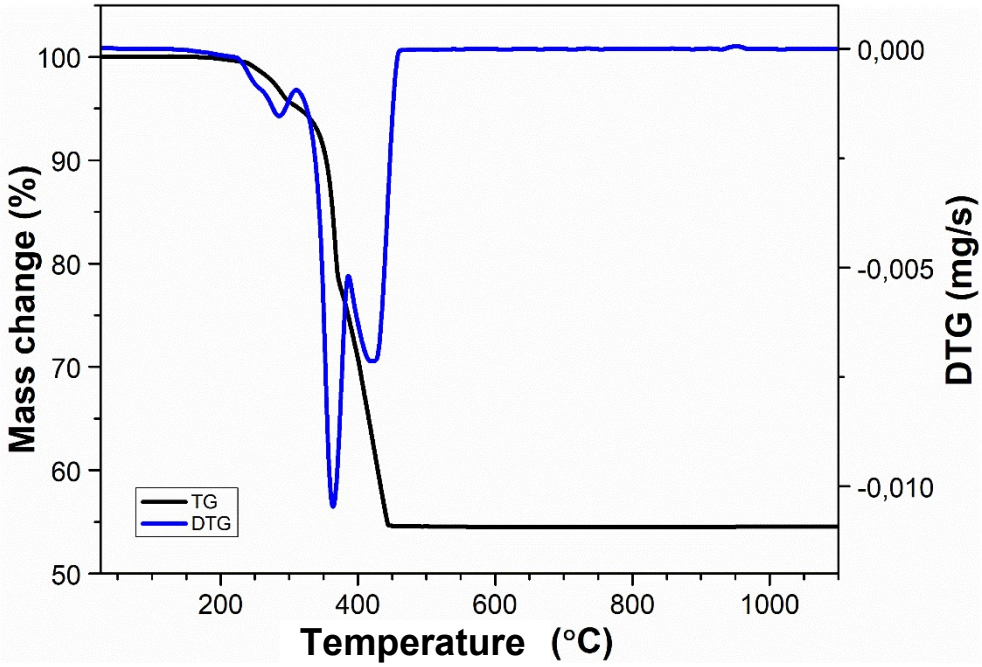

Figure S20. TG/DTG plot for **5**.

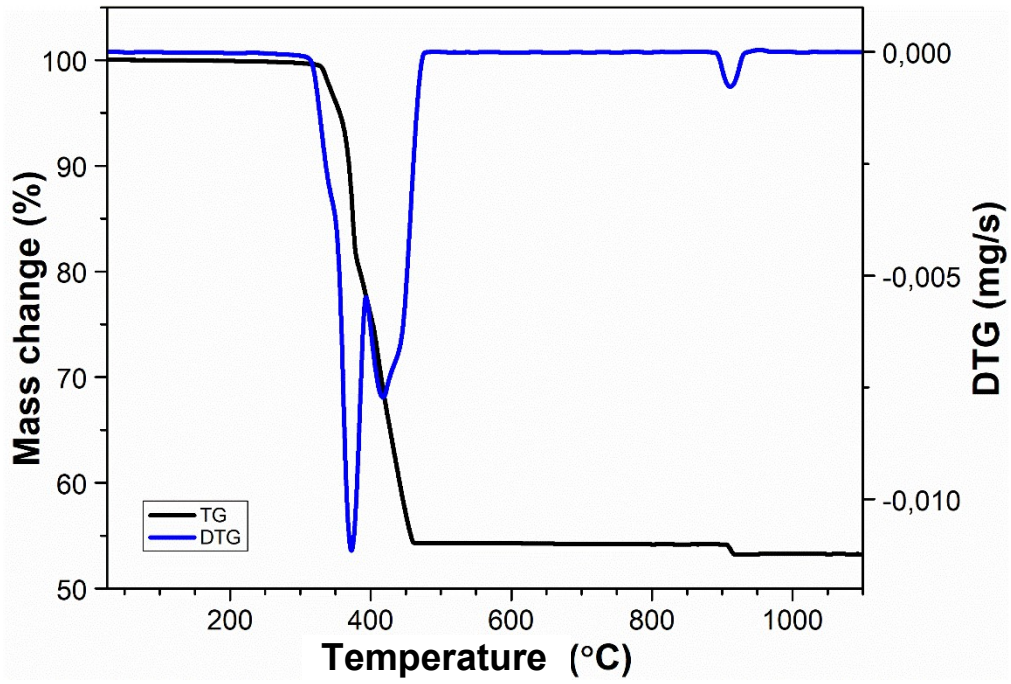

Figure S21. TG/DTG plot for **6**.

Catalysis: oxidation of phenylethanol to acetophenone in the presence of bimetallic metal imidazolates

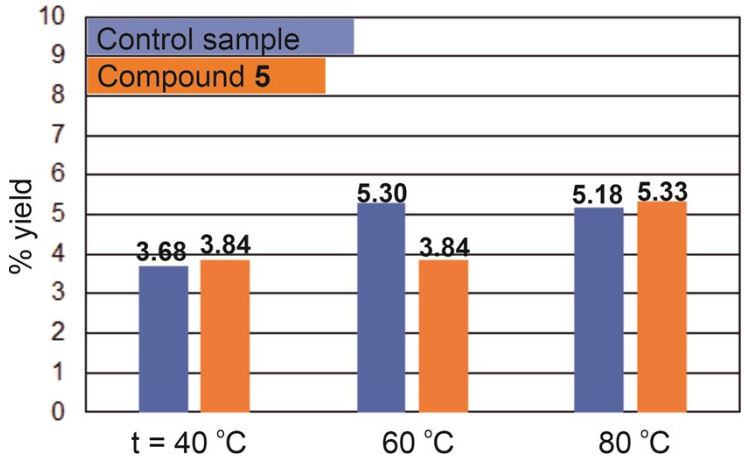

Figure S22. Influence of the addition of imidazolate **5** onto the yield of the reaction between the *tert*-butyl peroxide and 1-phenylethanol at three different temperatures. Each sample with the individual control. The yield of the reaction with the addition of 0.0290 g of **5** per 0.605 ml pf 1-phenylethanol (see Experimental).

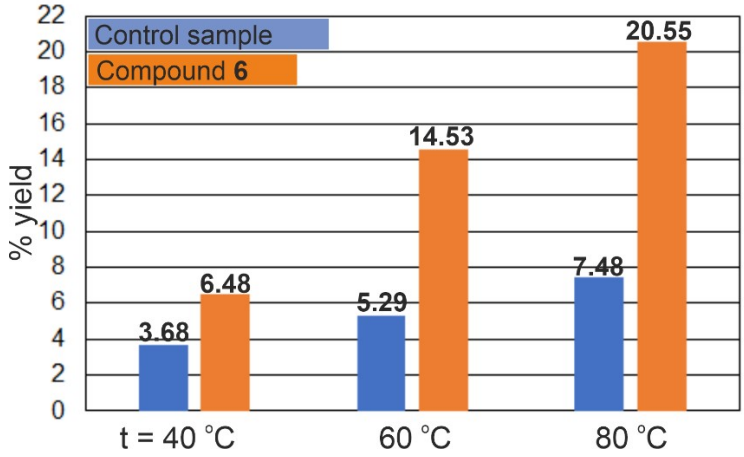

Figure S23. Influence of the addition of imidazolate **6** onto the yield of the reaction between the *tert*-butyl peroxide and 1-phenylethanol at three different temperatures. Each sample with the individual control. The yield of the reaction with the addition of 0.0290 g of **5** per 0.605 ml of 1-phenylethanol (see Experimental).

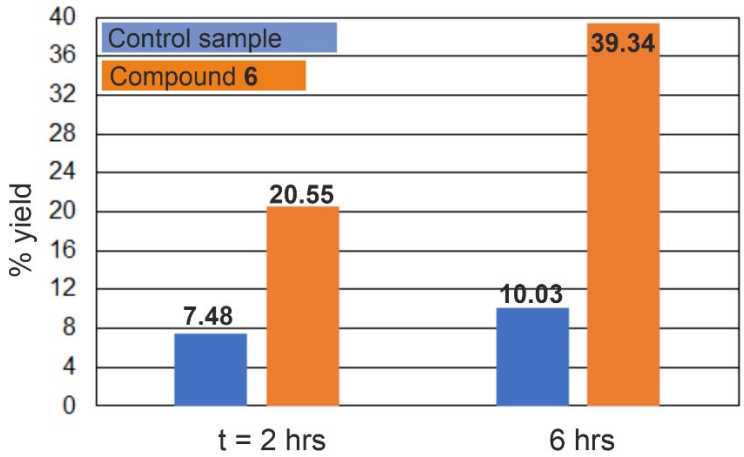

Figure S24. Influence of the addition of imidazolate **6** onto the yield of the reaction between the *tert*-butyl peroxide and 1-phenylethanol at two different times of . Each sample with the individual control. The yield of the reaction with the addition of 0.0290 g of **5** per 0.605 ml of 1-phenylethanol (see Experimental).